

# A Study of Adsorption Behavior of 2,4-Dichlorophenoxyacetic Acid onto Various GACs

Sook Jin Kim, Tae Young Kim, Seung Jai Kim<sup>†</sup> and Sung Yong Cho\*

Department of Environmental Engineering, \*RRC for Photonics Materials and Devices,  
Chonnam National University, Gwangju 500-757, Korea

(Received 4 April 2002 • accepted 20 May 2002)

**Abstract**—Adsorption and desorption of 2,4-dichlorophenoxyacetic acid (2,4-D) onto granular activated carbon (GAC) were studied to get basic information on their removal from aqueous solution. Single species adsorption equilibria of 2,4-D dissolved in water have been measured using F400, SLS103, and WWL. Equilibrium capacity increased with decreasing pH. The magnitude of adsorption capacity of 2,4-D was the order of F400>SLS103>WWL. Kinetic parameters were measured in a batch adsorber to analyze the adsorption rate of 2,4-D. The internal diffusion coefficients were determined by comparing the experimental concentration curve with that predicted from the surface diffusion model (SDM) and Pore diffusion model (PDM). The linear driving force approximation (LDFA) model was used to simulate isothermal adsorption behaviors in a fixed bed adsorber and successfully simulated experimental adsorption breakthrough behavior under various operation conditions.

Key words: Adsorption, Activated Carbon, 2,4-Dichlorophenoxyacetic Acid, Equilibrium, Batch Adsorption, Fixed Bed

## INTRODUCTION

Among the numerous agrochemicals in use today, the 2,4-dichlorophenoxy acetic acid (2,4-D), a member of the phenoxy herbicide group, has been widely applied to control broad leaf weeds. 2,4-D is a regulated compound due to its toxicity; solids containing 2,4-D in excess of 1,000 ppm are classified as hazardous. 2,4-D is used as agricultural herbicide against broad leaf weeds in cereal crops as well as on pastures and lawns, in parks, and on golf courses [Chen and Wang, 2000].

Various treatment techniques have been employed to treat the wastewater, including precipitation, adsorption, ion exchange, and reverse osmosis [Khan et al., 1997]. Among them, adsorption onto solid adsorbents has environmental significance, since it can effectively remove pollutants from wastewater. In wastewater treatment, activated carbon is a powerful adsorbent because it has a large surface area and pore volume, which allows the removal of liquid-phase contaminants, including organic compounds, heavy metal ions and colors [Hornsby et al., 1996; Kim et al., 2001]. The pollutant content, pH, and temperature of wastewater are likely to vary with time, so design of suitable adsorption systems is not that simple. This difficulty is compounded by the fact that the influence of these variables on the equilibrium amount of adsorption has not been extensively studied. In order to effectively design activated carbon adsorption units and to develop mathematical models that can accurately describe their operation, information on both the adsorption and the desorption of individual pollutants under different operating conditions is required [Buckingham, 1988; Kim and Suh, 1999; Markovska et al., 2001].

In this work, the main idea is to select a proper adsorbent for separation of 2,4-D from its aqueous solution and to find its adsorp-

tion and desorption characteristics by conducting experimental and theoretical work. Equilibrium data are experimentally measured and isotherm parameters are determined by employing some typical single species isotherm equations such as Langmuir, Freundlich and Sips. Particularly the effect of pH and temperature on equilibrium will be extensively discussed. Kinetic part is how to determine the kinetic model parameters, namely axial dispersion coefficient, external mass transfer coefficient and internal diffusion coefficient. These coefficients are major factors controlling rates of adsorption from solution by porous adsorbents. In general, the axial dispersion coefficient and the film mass transfer coefficient were determined by literature correlations. In order to determine the internal diffusion coefficient, a surface diffusion model (SDM) and pore diffusion model (PDM) were used for the prediction of adsorption breakthrough curves.

Adsorption and desorption on F400 were carried out to select for separating of 2,4-D. In order to demonstrate the applicability of the model under different operative conditions, fixed bed experiments were conducted by using different flow rate, initial pH, initial concentration, bed length, adsorbents.

## THEORETICAL APPROACH

### 1. Equilibrium Isotherm

Adsorption mechanisms are so complicated that no simple theory can adequately represent all experimental data. Many expressions have been published to describe the equilibrium relationship between the adsorbate and the adsorbent (activated carbon) most commonly used [Buckingham, 1988]. Some of the well-known adsorption isotherms for single-species systems are listed in Table 1.

To find the isotherm parameters for each adsorption, the equations were determined by using a linear least squares method and pattern search algorithm. The value of the mean percentage error has been used as a test criterion for the fit of the correlation. The mean percent deviation between experimental and predicted amount adsorbed is as follows:

<sup>†</sup>To whom correspondence should be addressed.

E-mail: sjkim@chonnam.ac.kr

<sup>\*</sup>This paper is dedicated to Professor Dong Sup Doh on the occasion of his retirement from Korea University.

**Table 1. Various isotherm models for single component system**

Isotherm	Model equations	Parameters
Langmuir	$q = \frac{q_m b C}{1 + b C}$	$q_m, b$
Freundlich	$q = k C^{1/n}$	$k, n$
Sips	$q = \frac{q_m b C^{1/n}}{1 + b C^{1/n}}$	$q_m, b, n$

$$\text{Error}(\%) = \frac{100}{N} \sum_{k=1}^N \left[ \frac{|q_{\text{exp},k} - q_{\text{cal},k}|}{q_{\text{exp},k}} \right] \quad (1)$$

### 1-1. Effect of Temperature

For useful description of adsorption equilibrium data at various temperatures, it is important to have the temperature dependence form of an isotherm equation [Zumriye and Julide, 2001].

The temperature dependence of the Sips equation is

$$q = \frac{q_m b C^{1/n}}{1 + b C^{1/n}} \quad (2)$$

for the affinity constant  $b$  and the exponent  $n$  may take the following form:

$$b = b_0 \exp\left(\frac{-\Delta H \cdot Z}{R}\right) \quad (3)$$

$$Z = \frac{1}{T} - \frac{1}{T_m} \quad (4)$$

Here,  $b_0$  is the adsorption affinity constant at mean temperature,  $T_m$ . The temperature dependence of the affinity constant  $b$  is taken from that of the Langmuir equation. Unlike in the Langmuir equation, where it is the isosteric heat, invariant with the surface loading, the parameter in the Sips equation is only the measure of the adsorption heat.

This temperature dependence form of the Sips equation can be used to fit adsorption equilibrium data of various temperatures simultaneously to yield the parameter  $b_0$ , and  $q_m$ .

### 1-2. Effect of Initial pH

The surface heterogeneity and chemical nature of the adsorbent surface are important factors for the determination of the influence of pH on the adsorption of single systems. Each experimental isotherm was plotted in terms of Sips equation to obtain the pH dependent parameters,  $q_m$  and  $b$  from Eq. (2).

The maximum adsorption amount  $q_m$ , the affinity constant  $b$  and the exponent  $n$  may take the following form:

$$q_m = q_{m0} \exp(\alpha \cdot Z) \quad (5)$$

$$b = b_0 \exp(-\beta \cdot Z) \quad (6)$$

$$Z = \frac{1}{\text{pH}} - \frac{1}{\text{pH}_m} \quad (7)$$

Here,  $b_0$  is the adsorption affinity constant at mean pH,  $\text{pH}_m$ , and are parameters of Sips of pH dependency equation.

## 2. Fixed Bed

It is assumed that adsorption occurs instantaneously and equilibrium is established between adsorbates in the fluid and on the surface of adsorbents. The driving force is the concentration gradient

of the adsorbate between liquid bulk and pore walls. The adsorbed species then diffuse into the pores in the adsorbed state. Provided that surface diffusion is dominant, the following equation can be expressed to describe the rate of adsorption for a spherical particle as [Kim et al., 2001]

$$\frac{\partial q}{\partial t} = \frac{3k_f}{R\rho_p} (C - C_s) = k_s (q_s - q) \quad (8)$$

The mass balance equation in the column and the relevant initial and boundary conditions are

$$-D_L \frac{\partial^2 C_i}{\partial z^2} + \frac{\partial v C_i}{\partial z} + \frac{\partial C_i}{\partial t} + \frac{1 - \epsilon_b}{\epsilon_b} \frac{\partial q_i}{\partial t} = 0 \quad (9)$$

$$C_i(z, t=0) = 0 \quad (10)$$

$$D_L \frac{\partial C_i}{\partial z} \Big|_{z=0} = -v(C_i|_{z=0} - C_i|_{z=0}) \quad (11)$$

$$\frac{\partial C_i}{\partial z} \Big|_{z=L} = 0 \quad (12)$$

## 3. Numerical Analysis

The most commonly used procedure for solving a set of partial differential equations (PDEs) is the finite difference method. This method requires quite strict conditions for stability. With an implicit scheme, many PDEs can be solved, but the stability condition strongly depends on parameter sensitivities.

In this study, the classical procedure of orthogonal collocation combined with the high accuracy of the finite element method was applied. The entire column is at first divided into a finite number of elements, in which the space variables are discretized by using the orthogonal collocation method [Lee, 1996]. The resulting set of the ordinary differential equations was then integrated numerically in the time domain by LSODI employing Gear's stiff method with variable order and step size.

## EXPERIMENTAL

The adsorbents used in this study were granular activated carbon (GAC) F400, SLS103 and WWL manufactured by Calgon, Samchully and Union Carbon Co., respectively. GAC, which was used as the adsorbent, was sieved into a narrow range of particle sizes (0.055-0.065 cm in dia.), before being washed with distilled water a few times to remove impurities and carbon powder and then stored after drying in the vacuum oven at 120 °C for 24 hr. The GACs were then stored in a sealed bottle along with a silica gel to prevent the re-adsorption of moisture before use. The physical properties of F400, SLS103 and WWL are listed in Table 2, respectively.

The adsorbates investigated were 2,4-D. The purity and manufacturer of 2,4-D is 99.0% (Acros Co.). All chemicals were used as received without further treatment. The solution pH was adjusted to 3.5, 7.0, 10.0 by the addition of NaOH and HCl. The solution pH, however, was not controlled during the adsorption process.

### 1. Isotherm Test

Adsorption isotherms were determined by contacting a volume (200 ml) of solution of 100 mg/l with a carefully weighed amount of GAC in a conical flask. The amount of carbon was varied (0.001-0.25 g) in single solute test. The flasks were continually shaken for

**Table 2. Properties of adsorbents**

Physical properties	Unit	F400	SLS103	WWL
Type	-	Coal-based	Coconut-based	Coal-based
Particle diameter	mm	0.37-0.54	0.37-0.54	0.37-0.54
Particle density	kg/m <sup>3</sup>	682	880	707
Particle porosity	-	0.62	0.47	0.57
BET surface area	m <sup>2</sup> /g	800	1040	670
Micropore area	m <sup>2</sup> /g	490	930	360
Average pore diameter	Å	19.02	15.11	15.44

7 days to provide good mixing and contact for equilibrium between the solid and liquid phase.

Concentration of solution of 2,4-D was determined with a UV-spectrophotometer (Shimadzu 1601) at  $\lambda=284$  nm. The amount of 2,4-D onto the GAC at equilibrium was calculated from the mass balance equation as follows:

$$q = (C_i - C) \frac{V}{W} \quad (13)$$

Here  $q$  is the equilibrium amount adsorbed on the adsorbent (mol/kg),  $C_i$  is the initial concentration of bulk fluid (mol/m<sup>3</sup>),  $C$  is the equilibrium concentration of the solution (mol/m<sup>3</sup>),  $V$  is the volume of solution (m<sup>3</sup>), and  $W$  is the weight of adsorbent (kg).

## 2. Kinetic and Column Test

Kinetic adsorption experiments were conducted in a batch adsorber with four baffles. The rotor speed was kept approximately 400 rpm, so that the external mass transfer resistance would be negligible. All runs were carried out at a temperature of 25 °C.

The column tests were conducted in a water-jacketed pyrex column with inside diameter and length of 1.5 and 44 cm, respectively. The column was packed with beads to distribute the solution uniformly. The activated carbon with known dried weight was put into the column. Distilled water was pumped into the column from the bottom to remove air bubbles and to rinse the carbon. In adsorption cycle, 2,4-D solution was continuously fed to the top of the column until the column was saturated with the feed 2,4-D solution. The saturated column was then regenerated with distilled water. The column temperature for all the column tests was maintained at 25 °C. The effluent samples were intermittently collected by a frac-

tion collector and measured by the UV-spectrophotometer (Shimadzu 1601).

## RESULTS AND DISCUSSION

### 1. Equilibrium Isotherm

Adsorption isotherms play a key role in the design of the adsorption-based process for treatment of wastewater disposal. In this study,

**Table 4. Adsorption equilibrium constants of 2,4-D onto three different adsorbate in terms of pHs at 298 K**

pH	Isotherm	Parameter	F400	SLS103	WWL	
3.5	Langmuir	$q_m$	1.857	1.384	1.431	
		$b$	33.86	61.79	17.95	
		Error (%)	3.111	8.451	7.660	
	Freundlich	$k$	2.639	2.011	1.802	
		$n$	3.974	3.798	2.836	
		Error (%)	1.354	2.990	4.797	
	Sips	$q_m$	3.025	3.458	2.460	
		$b$	2.361	1.137	1.738	
		$n$	2.164	2.664	1.900	
	7.0	Langmuir	$q_m$	0.165	0.646	0.571
			$b$	40.69	38.32	6.502
			Error (%)	2.937	3.935	1.828
Freundlich		$k$	0.771	0.898	0.696	
		$n$	4.451	3.558	1.994	
		Error (%)	2.335	3.428	1.693	
Sips		$q_m$	0.747	1.393	1.012	
		$b$	7.324	1.345	1.405	
		$n$	1.623	2.447	1.423	
10.0		Langmuir	$q_m$	0.53	0.631	2.183
			$b$	83.83	24.28	0.405
			Error (%)	2.701	2.261	3.701
	Freundlich	$k$	0.589	0.761	0.698	
		$n$	6.819	3.836	1.104	
		Error (%)	2.011	2.203	3.943	
	Sips	$q_m$	0.629	0.753	1.453	
		$b$	6.584	6.515	0.686	
		$n$	2.156	1.464	0.958	
	Error (%)	0.270	1.163	3.805		

**Table 3. Adsorption equilibrium constants of 2,4-D onto F400 for different temperature (pH 3.5)**

Isotherm	Parameters	288K	298K	303K
Langmuir	$q_m$	2.047	1.857	1.396
	$b$	56.14	33.86	67.36
	Error (%)	3.566	3.111	8.712
Freundlich	$k$	2.485	2.369	2.292
	$n$	5.223	3.974	3.306
	Error (%)	0.839	1.354	1.968
Sips	$q_m$	3.498	3.025	3.688
	$b$	1.979	2.361	1.196
	$n$	2.811	2.164	2.426
Error (%)	0.760	1.020	0.349	

single component isotherm data were correlated by the well known Langmuir, Freundlich, and Sips equations. The adsorption of 2,4-D onto GACs - F400, SLS103, and WWL - was favorable type, and single adsorption equilibrium data could be represented by the three proposed isotherms. Among these isotherms, for single species, Sips isotherm was used to fit the experimental equilibrium data. The affinity between 2,4-D with GACs was in the following order: F400 > SLS103 > WWL. The estimated values of the adsorption parameters are summarized in Table 3-5.

**Table 5. The calculated parameters of Sips equation of pH dependency**

Adsorbates	Parameters	2,4-D
F400	$q_{m0}$	1.558
	a	9.219
	b	1.012
	$\hat{a}$	3.221
	n	3.192
	Error (%)	7.931
SLS103	$q_{m0}$	34.30
	a	11.45
	b	0.028
	$\beta$	6.081
	n	3.779
	Error (%)	5.002
WWL	$q_{m0}$	1.182
	a	8.476
	b	0.795
	$\beta$	0.340
	n	2.230
	Error (%)	8.861

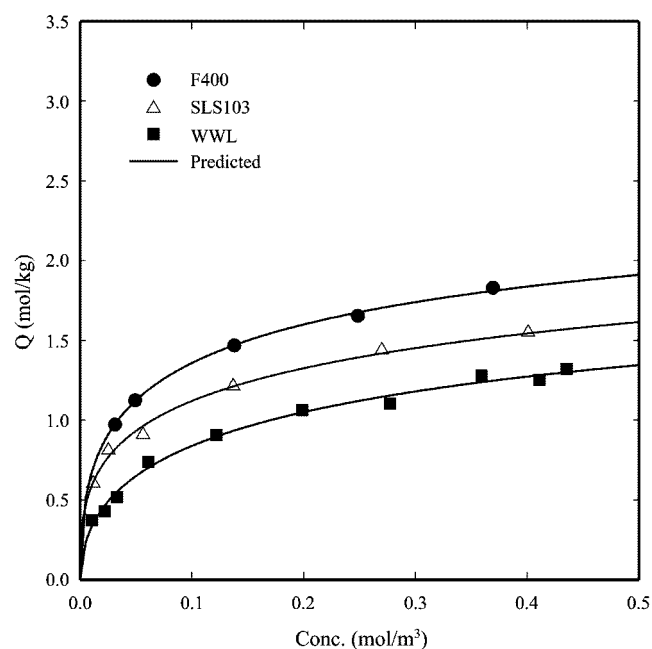


**Fig. 1. Adsorption equilibrium of 2,4-D onto three different adsorbents at initial pH of 3.5 and 298.15 K.**

## 1-2. Effect of Adsorbents

The surface chemistry of activated carbon and the chemical characteristics of adsorbate such as polarity, ionic nature, functional groups and solubility determine the nature of bonding mechanisms as well as the extent and strength of adsorption. A variety of physicochemical mechanisms forces, such as van der Waals, H-bonding, dipole-dipole interactions, ion exchange, covalent bonding, cation bridging and water bridging, can be responsible for adsorption of organic compounds in activated carbon [Zumriye and Julide, 2001].

The adsorption isotherms of 2,4-D onto three different adsorbents are shown in Fig. 1 at initial pH 3.5 and 298 K. As illustrated in this figure, the magnitude of adsorption capacity of 2,4-D was

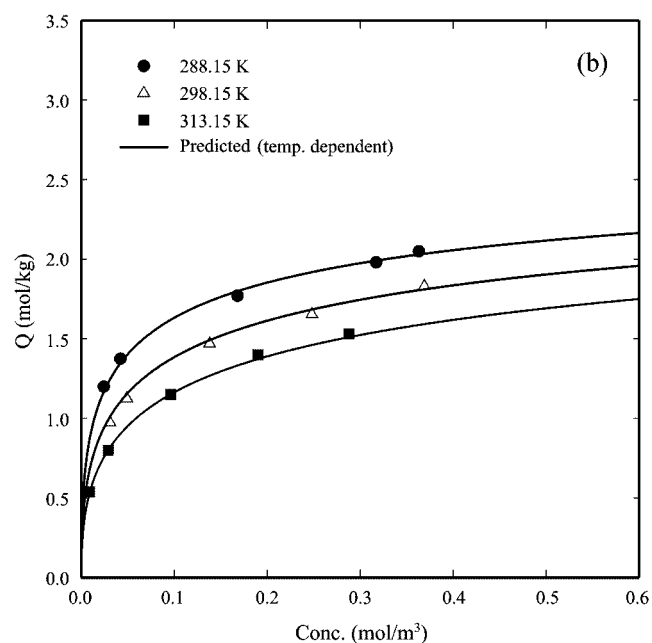
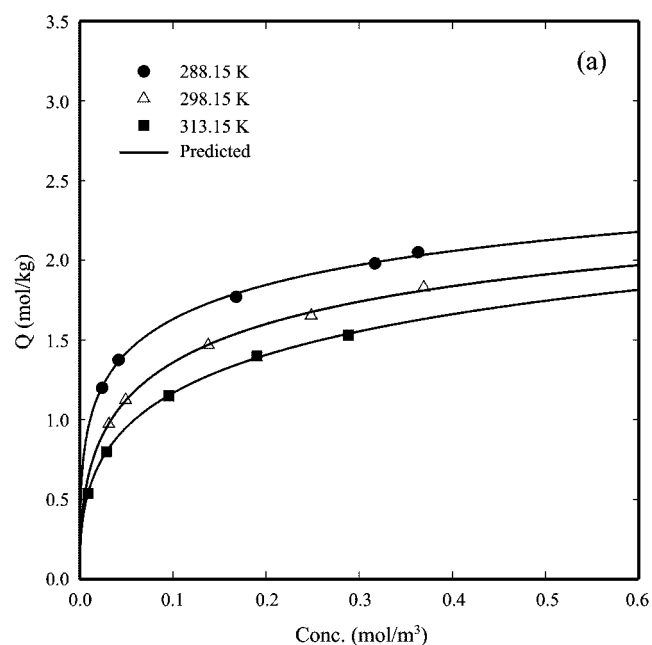


**Fig. 2. Experimental data and predicted adsorption isotherm for 2,4-D-F400 system for different temperatures at initial pH of 3.5 (a: Sips Eq., b: Temperature dependent Sips Eq.).**

the order of F400>SLS103>WWL. This result may come from the effect of the pore size distribution and the surface area, and surface properties.

### 1-3. Effect of Temperature

The effect of temperature on the adsorption isotherms of 2,4-D onto F400 adsorbate is shown in Fig. 2. The parameters of each isotherm were obtained by least square fitting with experimental data. These parameters and the average percent difference measured and calculated values are given in Table 3. In all cases there is a considerable effect of temperature and the isotherm becomes more linear as temperature is increased. Temperature has a significant effect on the adsorption isotherms. So we may conclude that physical ad-

sorption is dominant for adsorption system. In Fig. 2(b), the adsorption data for 2,4-D has been plotted with Sips of temperature dependency equation. The heat of adsorption for 2,4-D from aqueous solutions has been worked out. The values of heat of adsorption for 2,4-D was  $1.47 \times 10^4$  J/mol. The accuracy of the values is dependent on the degree of fitness, which can be judged by comparing average percentage error.

### 1-4. Effect of Initial pH

All of the constant pH adsorption isotherms show type adsorption isotherm behavior, with saturation capacities depending on pH. Figs. 3, 4 and 5 show the experimental equilibrium adsorption isotherms obtained at the different initial pHs for the adsorption of 2,4-

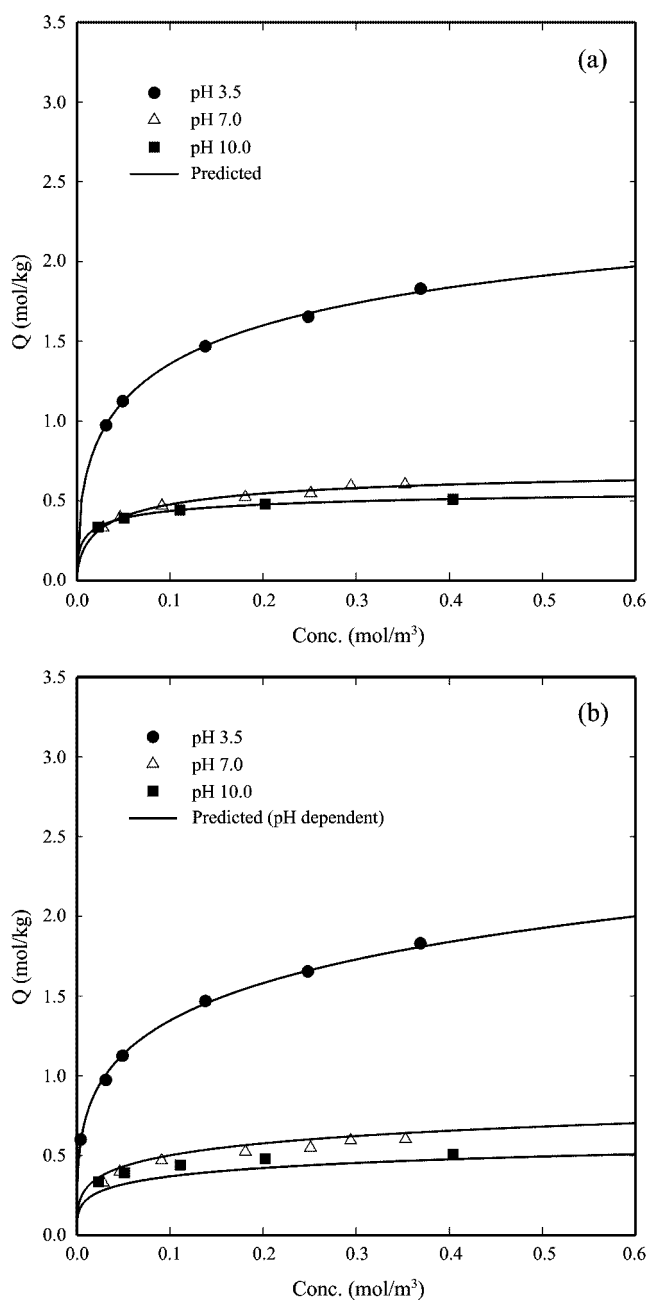


Fig. 3. Experimental data and predicted adsorption isotherm for 2,4-D-F400 system for different initial pH at 298.15 K (a: Sips Eq., b: pH dependent Sips Eq.).

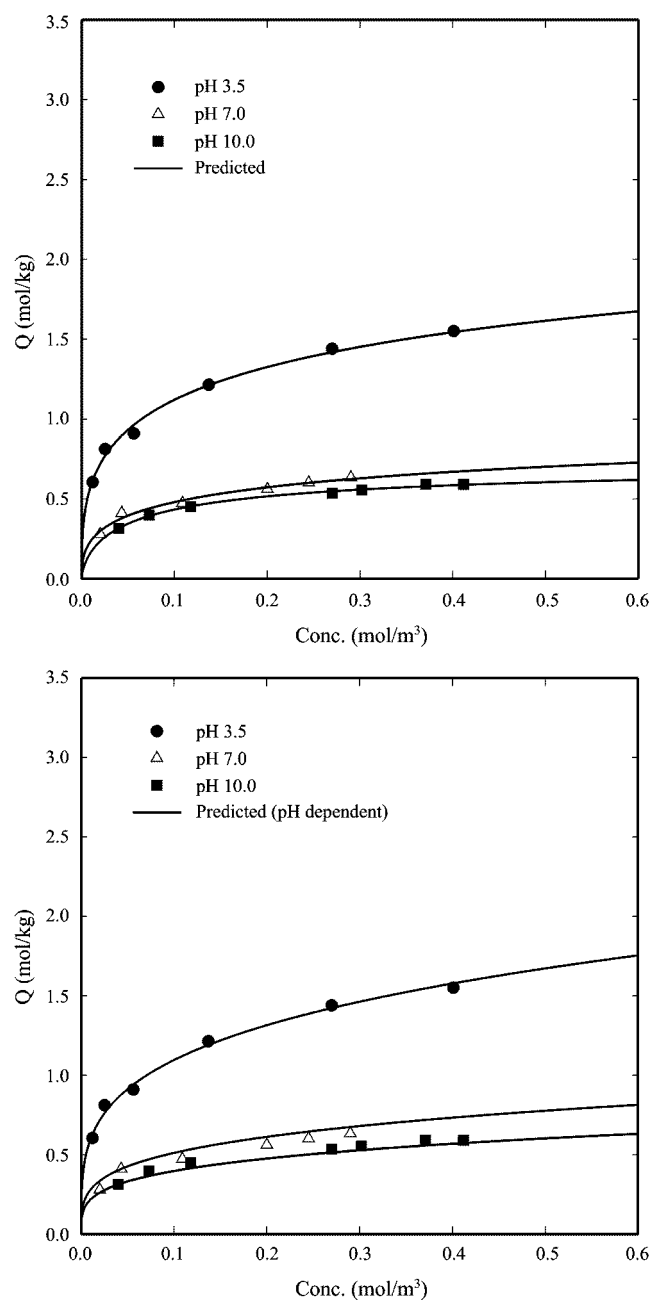


Fig. 4. Experimental data and predicted adsorption isotherm for 2,4-D-SLS103 system for different initial pH at 298.15 K (a: Sips Eq., b: pH dependent Sips Eq.).

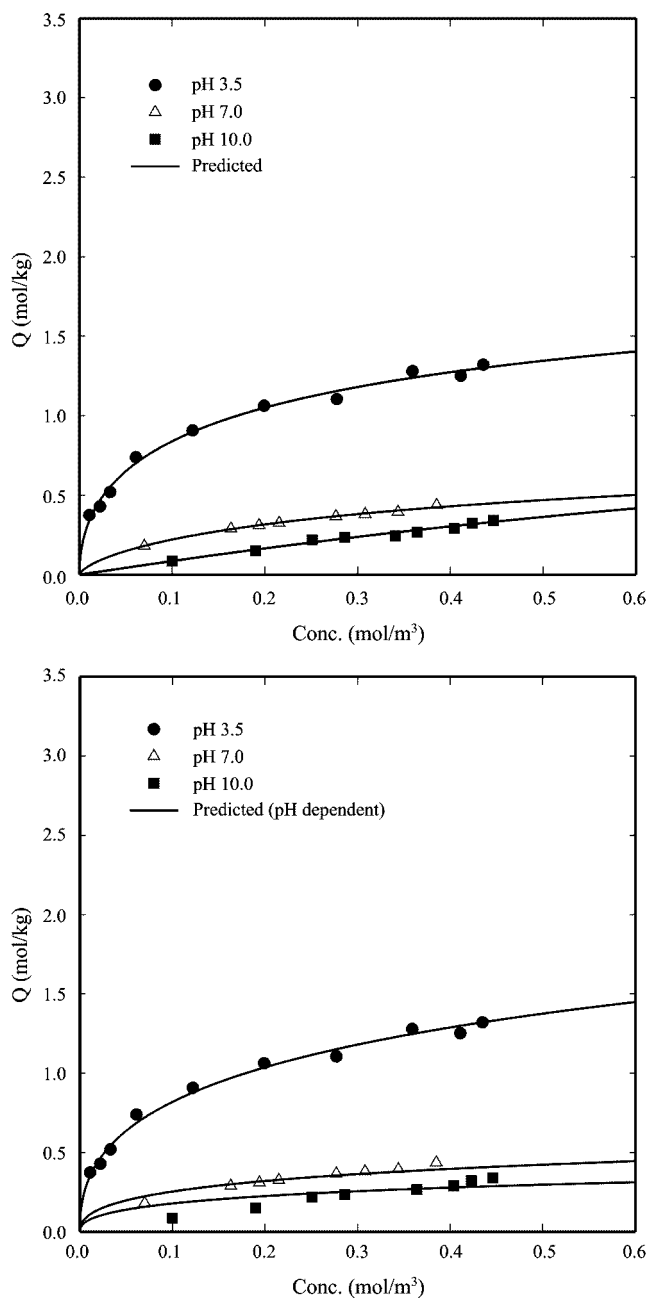


Fig. 5. Experimental data and predicted adsorption isotherm for 2,4-D-WWL system for different initial pH at 298.15 K (a: Sips Eq., b: pH dependent Sips Eq.).

D onto F400, SLS103, and WWL, respectively. As shown in those figures, the equilibrium adsorption amounts of 2,4-D onto three different adsorbents increased with decreasing solution pH. It is a common observation that anions are favorably adsorbed on the surface of adsorbents at low pH because the presence of hydrogen ions renders the surface active for the adsorption of cations at high pH values. The experimental data are well represented by the Sips equation (a) and pH dependent Sips equation (b). A Sips model and pH dependent parameters were fitted successfully for all of the pH conditions. The calculated parameters of pH dependent Sips equation are listed in Table 5. Compared with those in Table 4, the percent error differences between the Sips equation and pH dependent Sips

equation are not very large. So, we could correlate single-component isotherm data by the modified Sips equation. The choice of the pH dependent function is arbitrary.

In general, the influence of pH is attributed to the electrostatic interaction between the adsorbent surface and the adsorbate molecule or ion. This suggests that effective separation could be achieved by the adjustment of pH.

## 2. Batch Adsorption

The adsorption on a solid surface takes place in several steps, such as external diffusion, internal diffusion, and actual adsorption. Usually, the actual adsorption process is relatively fast compared to the previous two steps. Intraparticle diffusion has been usually considered as the rate-controlling step in liquid-phase adsorption. However, it is important to estimate the order of magnitude of the mass transfer coefficient. In this work, we estimated from the initial concentration decay curve when the diffusion resistance does not prevail.

The external film mass transfer coefficient,  $k_f$ , can be obtained from the experimental data by plotting the  $\ln(C/C_i)$  vs.  $t$ , in which time range is zero to 300 seconds [Misic et al., 1977].

$$\ln(C/C_i) = -k_f A_s t / V_s \quad (14)$$

where  $V_s$  is the volume of solution and  $A_s$  is the effective external surface area of adsorbent particles,

$$A_s = 3W / \rho_p R_p \quad (15)$$

Fig. 6 shows the experimental data and model prediction for the adsorption of 2,4-D for three different adsorbents in a batch adsorber. In this study, the pore diffusion coefficient,  $D_p$ , and surface diffusion coefficient,  $D_s$ , are estimated by pore diffusion model (PDM) and surface diffusion model (SDM) [Moon and Lee, 1983]. The estimated values of  $k_f$ ,  $D_p$ , and  $D_s$  for 2,4-D are listed in Table 6,

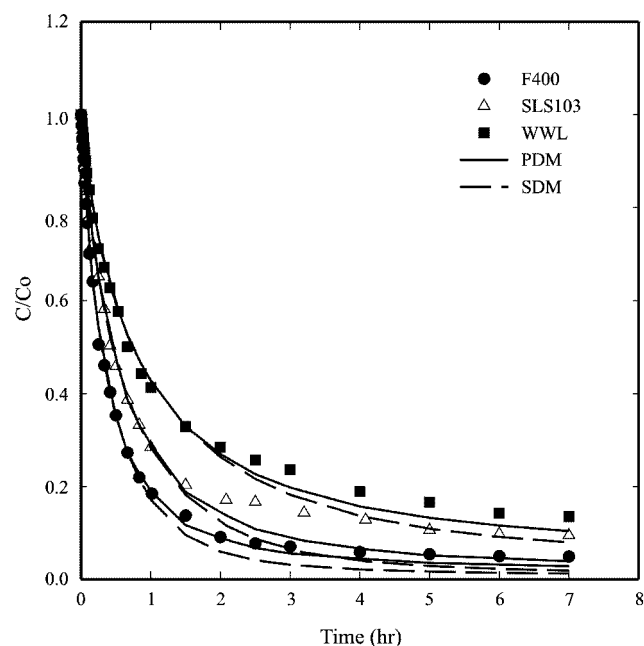


Fig. 6. Observed and predicted uptake curves of 2,4-D onto three different adsorbents at 298.15 K and initial pH of 3.5 (volume of the solution=1 L and amount of GAC=1 g).

**Table 6. Kinetic parameters onto three different adsorbents in a batch reactor**

Adsorbents	Adsorbates	$k_f \times 10^5$ m/sec	$D_s \times 10^{13}$ m <sup>2</sup> /sec	$D_p \times 10^9$ m <sup>2</sup> /sec
F400	2,4-D	5.00	1.90	1.42
SLS103	2,4-D	4.17	1.85	1.50
WWL	2,4-D	2.53	1.58	0.62

which shows the magnitude of the three estimated values,  $D_s$  being much smaller than other two. This implies that the diffusion inside a particle is a rate-controlling step.

### 3. Fixed Bed Adsorption

For a packed bed adsorber, the main parameters for mass transfer are the axial dispersion coefficient and the external film mass transfer coefficient. Axial dispersion contributes to the broadening of the adsorption front axially due to flow in the interparticle void spaces. Usually it comes from the contribution of molecular diffusion and the dispersion caused by fluid flow. In this study, the axial dispersion coefficient, for the fixed bed adsorber was estimated by Wakao's correlation [1978].

$$\frac{D_L}{2\nu R_p} = \frac{20}{\xi} \left( \frac{D_m}{2\nu R_p} \right) + \frac{1}{2} = \frac{20}{\text{ReSc}} + \frac{1}{2} \quad (16)$$

External film mass transfer is that by diffusion of the adsorbate molecules from the bulk fluid phase through a stagnant boundary layer surrounding each adsorbent particle to the external surface of the solid. The external film mass transfer coefficient,  $k_f$ , in a fixed bed adsorber can be estimated by the Wakao and Funazkri equation [1978].

$$k_f = \frac{D_m}{2R_p} (2.0 + 1.1 \text{Re}^{0.6} \text{Sc}^{0.33}) \quad (17)$$

where Sc and Re are Schmidt and Reynolds numbers, respectively. In Eqs. (16) and (17), molecular diffusion coefficients,  $D_m$ , of 2,4-D can be calculated by the Wilke-Chang equation [Reid et al., 1994].

The dynamic studies of 2,4-D onto GAC were carried out in a fixed-bed. For these systems, the data were fitted by LDFA model. The changes in other parameters such as flow rates, and adsorbents (F400, SLS103, and WWL) showed that the breakthrough times were shifted in the axis of time. The experimental conditions for fixed bed adsorption are shown in Table 9.

Since the flow rate is an important factor in a fixed bed design, its effects were studied by testing different fluid velocities. Fig. 7 shows that the breakthrough time was shorter for higher flow rate. Usually, the intraparticle diffusivity is believed to be independent of flow rate. However, the breakthrough curves were found to be steeper at higher flow rate as shown in Fig. 7. This phenomenon is

**Table 7. Experimental conditions for fixed-bed adsorption**

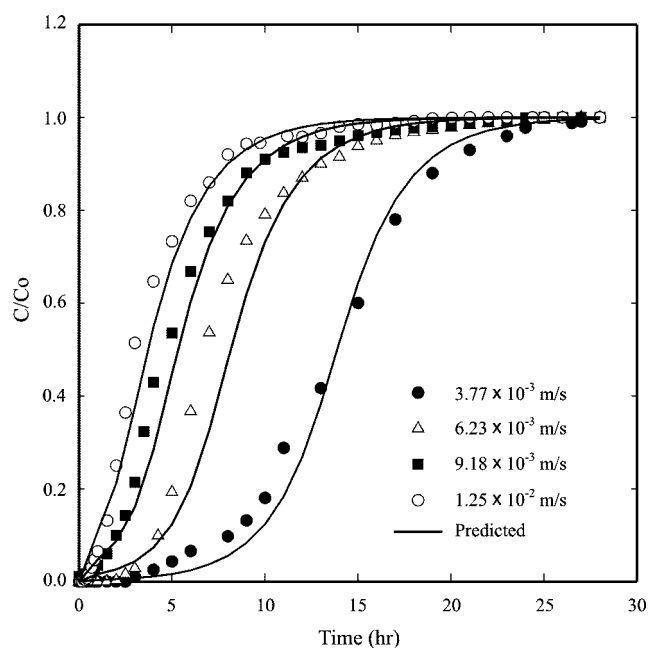
Variables	Unit	Experimental conditions
Bed length (L)	m	0.06 0.15
Bed diameter (D)	m	0.015
Bed density	kg/m <sup>3</sup>	385 538
Flow rate ( $\nu$ )	m/s	$3.77 \times 10^{-3} \sim 1.25 \times 10^{-2}$
Temperature	K	298
Initial pH	-	3.5, 7.0, 10.0

attributed to external film mass transfer resistance. This resistance is smaller when flow rate is higher, so that the length of mass transfer zone is reduced and a sharper breakthrough curve is generated.

Fig. 8 shows the experimental data and model predictions of breakthrough curves for different GAC. The mass of adsorbent is 0.01 kg and packed bed height of F400, SLS103, and WWL is 0.10 m, 0.12 m, and 0.14 m, respectively. This means that the bed porosity of F400 is the smallest. As shown in Fig. 1, since the adsorption capacity of 2,4-D onto F400 is greater than the other two adsorbents, the breakthrough time of 2,4-D onto F400 was increasing. For the successful application of an adsorption system, an efficient regeneration of the used adsorbent is very important from the economic point of view. In general, there are many regeneration techniques such as thermal, steam, acid or base and solvent regenerations. The choice of a certain regeneration method should depend upon the physical and chemical characteristics of both the adsor-

**Table 8. Values of parameter for fixed-bed model simulation as flow rates**

Superficial velocity (m/sec)	$k_f \times 10^5$ (m/sec)	$D_L \times 10^5$ (m <sup>2</sup> /sec)
$3.77 \times 10^{-3}$	2.78	1.79
$6.23 \times 10^{-3}$	3.67	2.98
$9.18 \times 10^{-3}$	4.56	4.40
$1.25 \times 10^{-2}$	5.43	6.00

**Fig. 7. Effect of flow rate on experimental results and model predictions of breakthrough curves for 2,4-D onto F400 (T=298.15 K, C<sub>0</sub>=100 mg/l, L=0.10 m, and initial pH of 3.5).**

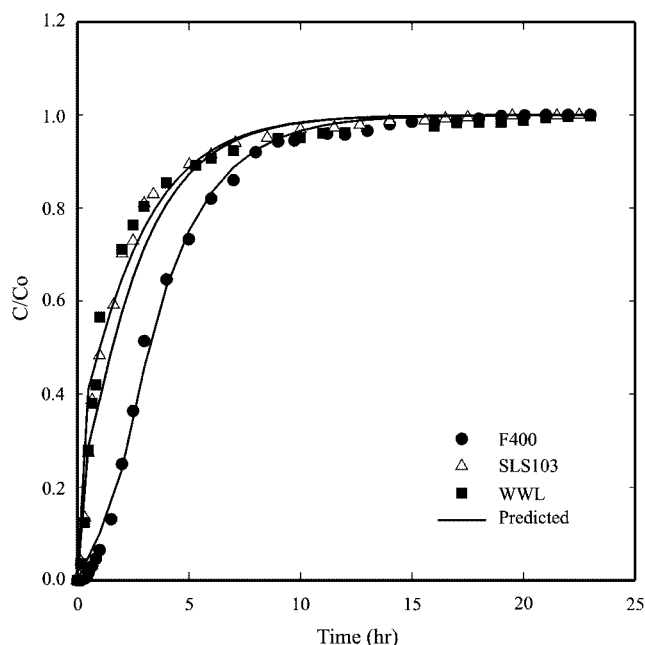


Fig. 8. Experiment data and model predictions of breakthrough curves for different GAC (Adsorbate: 2,4-D,  $T=298.15$  K,  $C_0=100$  mg/l,  $v=1.25 \times 10^{-2}$  m/sec,  $pH_i=3.5$ ).

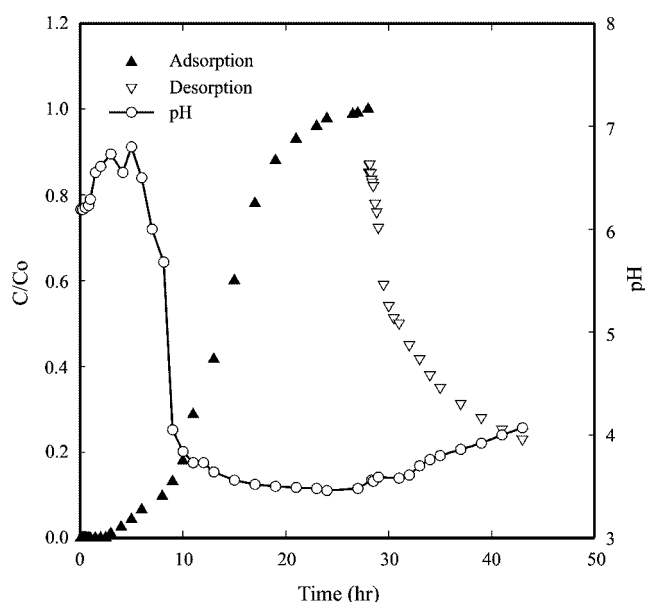


Fig. 9. pH variations during adsorption and desorption process for 2,4-D-F400 system ( $T=298.15$  K,  $C_0=100$  mg/l,  $v=3.77 \times 10^{-3}$  m/sec,  $L=0.10$  m,  $pH_i=3.5$ ).

bate and the adsorbent. In this study, distilled water was used as desorbate for GAC. As shown in Fig. 9, desorption of 2,4-D was about 80% only using distilled water of usually pH 6. The effluent pH decreased in the earlier adsorption stage, and then increased to influent pH as adsorption proceeded, as represented in Fig. 9. At pH 3.5 and 2,4-D concentration of 100 mg/l, the effluent pH sharply decreased up to about nearly 3.5 and then slowly increased. As discussed previously, the rapid decrease of effluent pH in the earlier adsorption stage also implies that large amounts of 2,4-D was re-

moved by an F400 with hydronium ions on the surface functional group [Lee, 1996]. As adsorption proceeds, the solution pH in a fixed bed increases and the adsorption amount becomes higher. Therefore, in order to predict the adsorption characteristics of 2,4-D in a fixed bed, the pH influence must be considered.

## CONCLUSION

The adsorption of 2,4-D onto GACs - F400, SLS103, and WWL - was favorable type, and single adsorption equilibrium data could be represented by the three proposed isotherms. Among these isotherms, for single species, the Sips isotherm was used to fit the experimental equilibrium data. A Sips model with pH dependent parameters was fitted successfully with experimental data for all of the initial pHs. The affinity between 2,4-D with GACs was in the following order: F400>SLS103>WWL.

A simple dynamic model (LDFA) successfully simulated the experimental adsorption breakthrough data under various operation conditions. In particular, the adsorption capacity of F400 for 2,4-D considerably decreased with the solution pH, for the pH range of 3.0-10.0. This implies that the affinity between the adsorbates and F400 depends strongly on the type of ionic forms. Though there are some deviations between experimental and simulated breakthrough curves, the adsorption method applied in this work for the treatment of coexistent ionic forms will be very useful in predicting the adsorption behavior, especially at low values of pH which is typical condition for treatment of aqueous solution containing 2,4-D.

## ACKNOWLEDGEMENT

The authors wish to acknowledge a grant in aid for research from the KRF (No. Y00316).

## NOMENCLATURE

- $A_s$  : surface area of the adsorbent particles [ $m^2$ ]
- $b$  : isotherm parameter
- $C$  : equilibrium concentration of the solution [ $mol/m^3$ ]
- $C_i$  : initial concentration of bulk fluid [ $mol/m^3$ ]
- $C_s$  : saturation concentration of the adsorbate in the liquid phase [ $mol/m^3$ ]
- $D_L$  : axial dispersion coefficient [ $m^2/sec$ ]
- $D_m$  : molecular diffusion coefficient [ $m^2/sec$ ]
- $k$  : isotherm parameter
- $k_f$  : film mass transfer coefficient [ $m/sec$ ]
- $k_s$  : solid mass transfer coefficient [ $sec^{-1}$ ]
- $n$  : isotherm parameter
- $pH_i$  : initial pH
- $q$  : equilibrium amount adsorbed on the adsorbent [ $mol/kg$ ]
- $q_i$  : concentration of bulk fluid [ $mol/kg$ ]
- $q_m$  : maximum adsorption capacity of adsorbent [ $mol/kg$ ]
- $q_s$  : concentration at the exterior surface of the particle [ $mol/kg$ ]
- $R_p$  : particle radius [ $m$ ]
- $T$  : temperature [ $K$ ]
- $t$  : time [ $sec, hr$ ]

V : volume of solution  
 $v_s$  : superficial velocity [ m/sec]  
 W : weight of adsorbent [kg]  
 z : axial distance [m]

#### Greek Letters

$\alpha$  : equilibrium constant of Sip equation of pH dependency  
 $\beta$  : equilibrium constant of Sip equation of pH dependency  
 $\rho_p$  : particle density [kg/m<sup>3</sup>]  
 $\epsilon_b$  : bed porosity  
 $\xi$  : voidage between granules (void fraction)

#### Abbreviation

GAC : granular activated carbon  
 PDM : pore diffusion model  
 Re : Reynolds number  
 Sc : Schmidt number  
 SDM : surface diffusion model

#### REFERENCES

- Buckingham, J., "Dictionary of Organic Compounds," 5th Ed. and Supplements, Chapman and Hall, New York, **2**, 2275 (1988).
- Chen, J. P. and Wang, X., "Removing Copper, Zinc, and Lead Ion by Granular Activated Carbon in Pretreated Fixed-bed Columns," *Sep. & Purifi. Tech.*, **19**, 157 (2000).
- Hornsby, A. G., Wauchope, R. D. and Herner, A. E., "Pesticide Properties in the Environment," Springer - Verlag New York, Inc. (1996).
- Khan, A. R., Atallah, R. and Al-Haddad, A., "Equilibrium Adsorption Studies of Some Aromatic Pollutants from Dilute Aqueous Solutions on Activated Carbon at Different Temperatures," *J. Colloid Interface Sci.*, **194**, 154 (1997).
- Kim, T. Y., Kim, S. J. and Cho, S. Y., "Effect of pH on Adsorption of 2,4-Dinitrophenol onto an Activated Carbon," *Korean J. Chem. Eng.*, **18**, 755 (2001).
- Kim, Y. M. and Suh, S. S., "A New Mass Transfer Model for Cyclic Adsorption and Desorption," *Korean J. Chem. Eng.*, **16**, 401 (1999).
- Lee, J. W., "Separation of Cephalosporin C in Nonionic Polymeric Resin Columns," PhD. Thesis, Department of chemical technology, Chonnam National University (1996).
- Markovska, L., Meshko, V. and Noveski, V., "Adsorption of Basic Dyes in a Fixed Column," *Korean J. Chem. Eng.*, **18**, 190 (2001).
- Misic, D. M., Sudo, Y., Suzuki, M. and Kawazoe, K. "Liquid to Particle Mass Transfer in a Stirred Batch Adsorption Tank with Nonlinear Isotherm," *J. Chem. Eng. Japan*, **15**, 490 (1977).
- Moon, H. and Lee, W. K., "Intraparticle Diffusion in Liquid-phase Adsorption of Phenols with Activated Carbon in Finite Batch Adsorber," *J. Colloid Interface Sci.*, **96**, 162 (1983).
- Reid, R. C., Prausnitz, J. M. and Pokung, B. E., "The Properties of Gases and Liquids," McGraw-Hill Co., New York (1994).
- Wakao, N. and Funazkri, "Effect of Fluid Dispersion Coefficient on Particle to Fluid and Mass Transfer Coefficients in Packed Bed," *Chem. Eng. Sci.*, **33**, 1375 (1978).
- Zumriye, A. and Julide, Y., "A Comparative Adsorption/biosorption Study of Mono-chlorinated Phenols onto Various Sorbents," *Waste Management*, **21**, 695 (2001).